SUPPLEMENTAL RESULTS

Supplemental Fig. 1

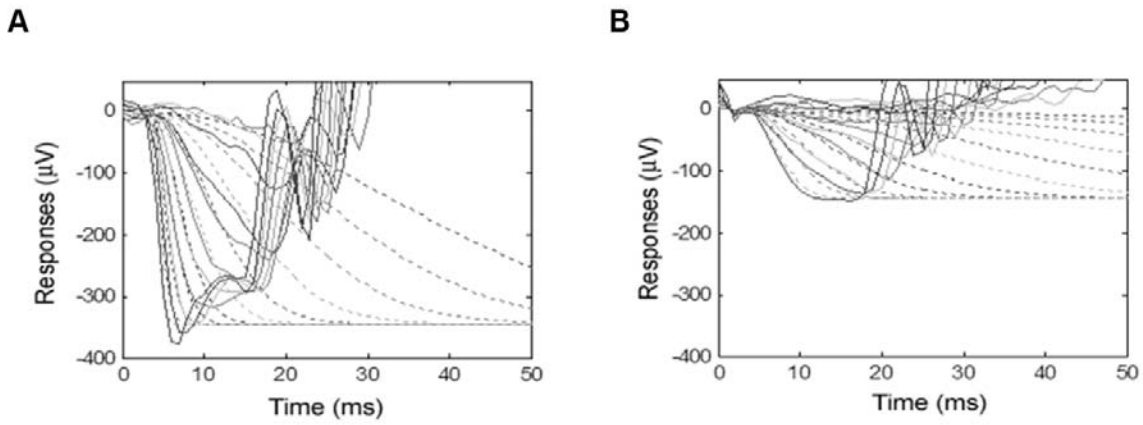

Supplemental Fig. 1. Representative a-wave responses from control (*A*) and *Cav-1* KO (*B*) fit to a computational model of phototransduction**.** Rod responses were elicited by flashes ranging in energy from 0.4-3.4 log scotopic td•s/m^2 in 0.3 log steps. The derived maximum a-wave amplitude (Rm_{p3}) was 373.0 ± 71.56 µV for controls and159.8 ± 57.62 µV for *Cav-1* KO mice. Sensitivity (log S), a measure of phototransduction gain, was 2.37 ± 0.14 s^{-2} $(td/s)^{-1}$ for controls and 1.28 ± 0.43 s^{-2} $(td/s)^{-1}$for *Cav-1* KO. Both Rmp3 and log S were significantly lower in *Cav-1* KO mice compared to controls ($p \leq 0.05$, Student's *t*-test, n = 5).

Supplemental Fig. 2

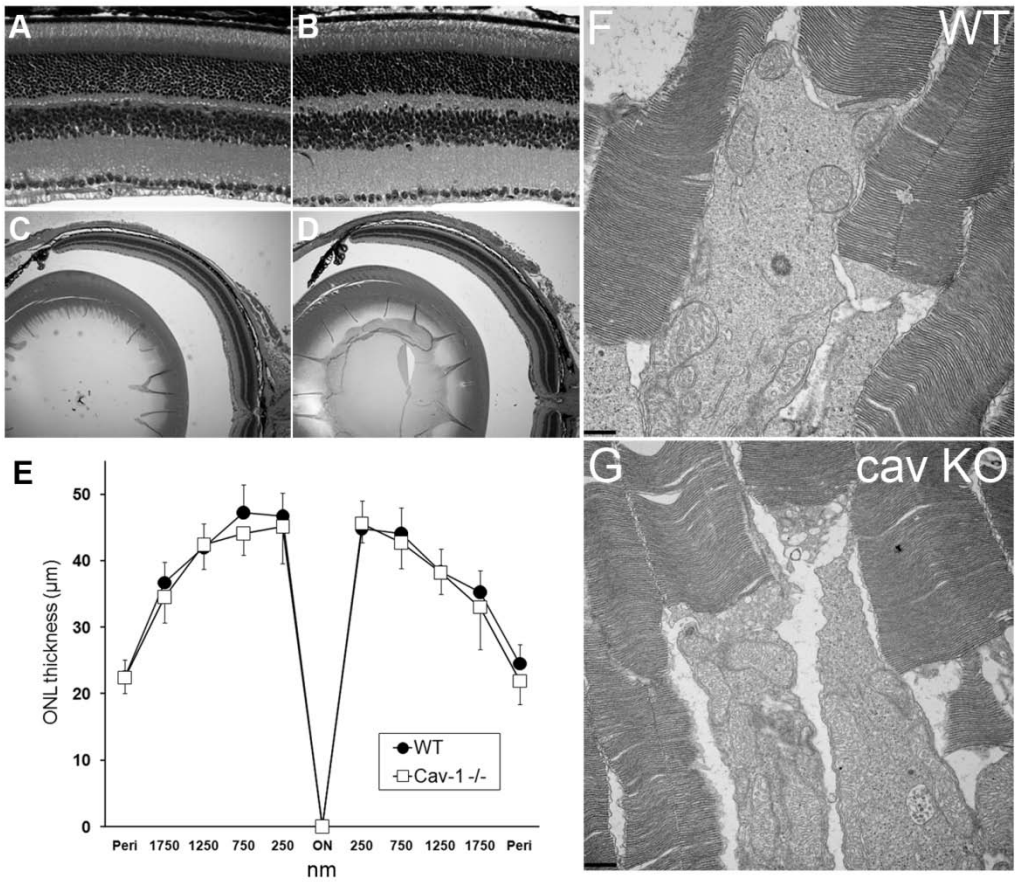

Supplemental Fig. 2. Retinal architecture in 8-week *Cav-1* KO mice was indistinguishable from controls. Representative H&E stained sections of WT (*A, C*) and *Cav-1* KO (*B, D*) retinas. Photoreceptor outer nuclear layer thickness (*E*) and photoreceptor ultrastructure (*F, G*) were normal in *Cav-1* KO mice. Scale bar in F, G is 500 nm.

Supplemental Fig. 3

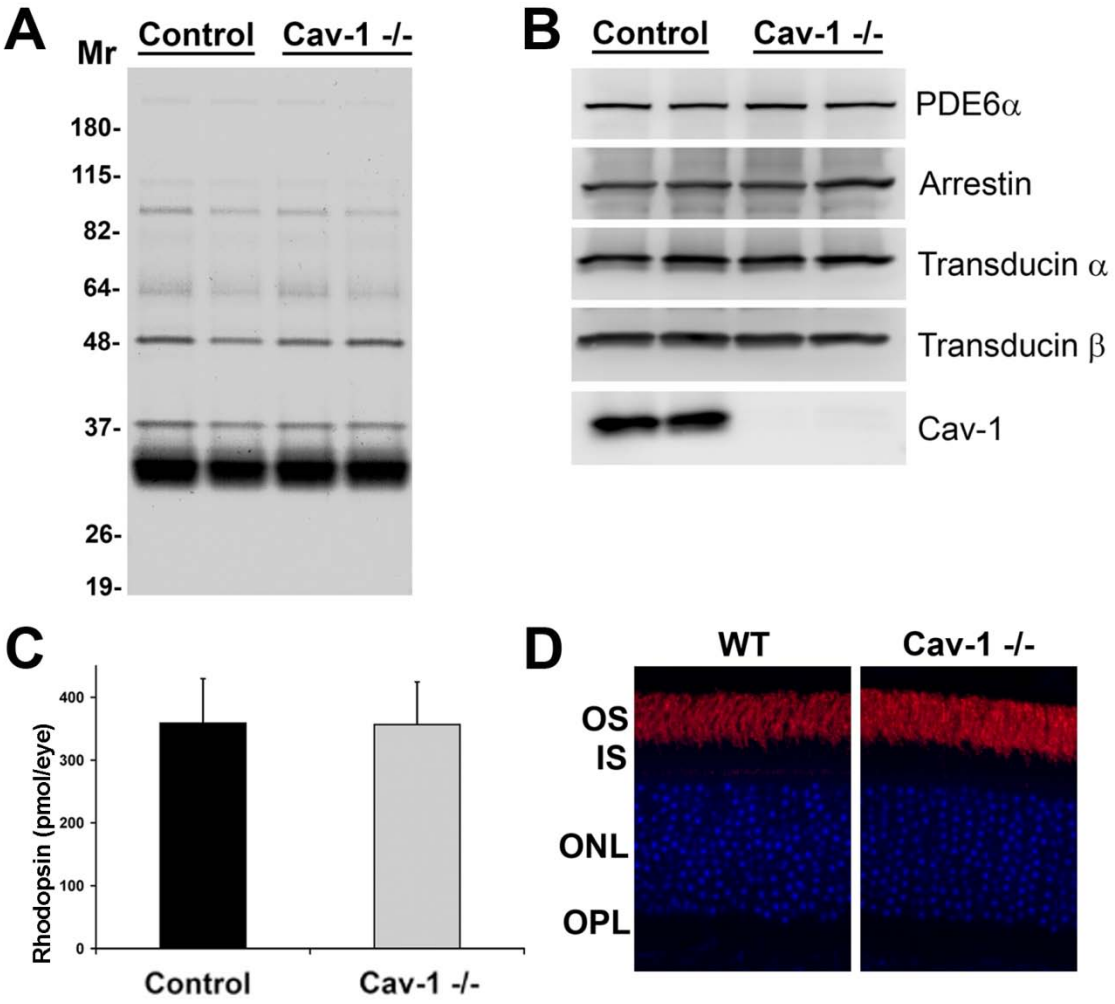

Supplemental Fig. 3. Analyses of rod phototransduction proteins in *Cav-1* KO retinas. (*A*) Purified ROS membranes from WT and *Cav-1* KO mice were subjected to SDS-PAGE and proteins were stained with Gelcode blue reagent. No differences in the protein profile of ROS membranes was observed. Whole retinal lysates were prepared and analyzed by Western blotting (*B*) analysis for PDE6α, Arrestin, Transducin α, Transducin β and Cav-1. No significant differences in the levels of any of these proteins were observed between the two groups. The levels of bleachable rhodopsin (*C*) measured spectrophotometrically from dark-adapted retinas was not significantly different between in *Cav-1* KO mice and controls (n = 7). The localization of rhodopsin (*D*) was also normal in *Cav-1* KO mice.

Supplemental Fig. 4.

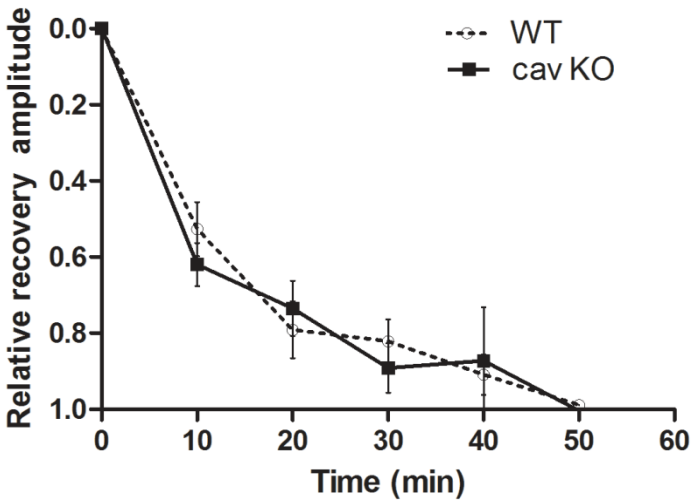

Supplemental Fig. 4. Recovery of a-wave responses after bleaching (steady illumination of 2.7 log cd/m^2 for 5 min) in control (circle, n=6) and *Cav-1* KO mice (rectangles, n = 6). A-wave response amplitudes before and after bleaching were elicited by a test flash of 2.3 log cd $\cdot$ s/m^2. A-wave responses at the indicated times after bleaching were normalized to the initial fully dark adapted responses and expressed as relative recovery. Loss of Cav-1 did not influence the rate of recovery after bleaching suggesting that the visual cycle was normal in *Cav-1* KO mice.

Supplemental Fig. 5.

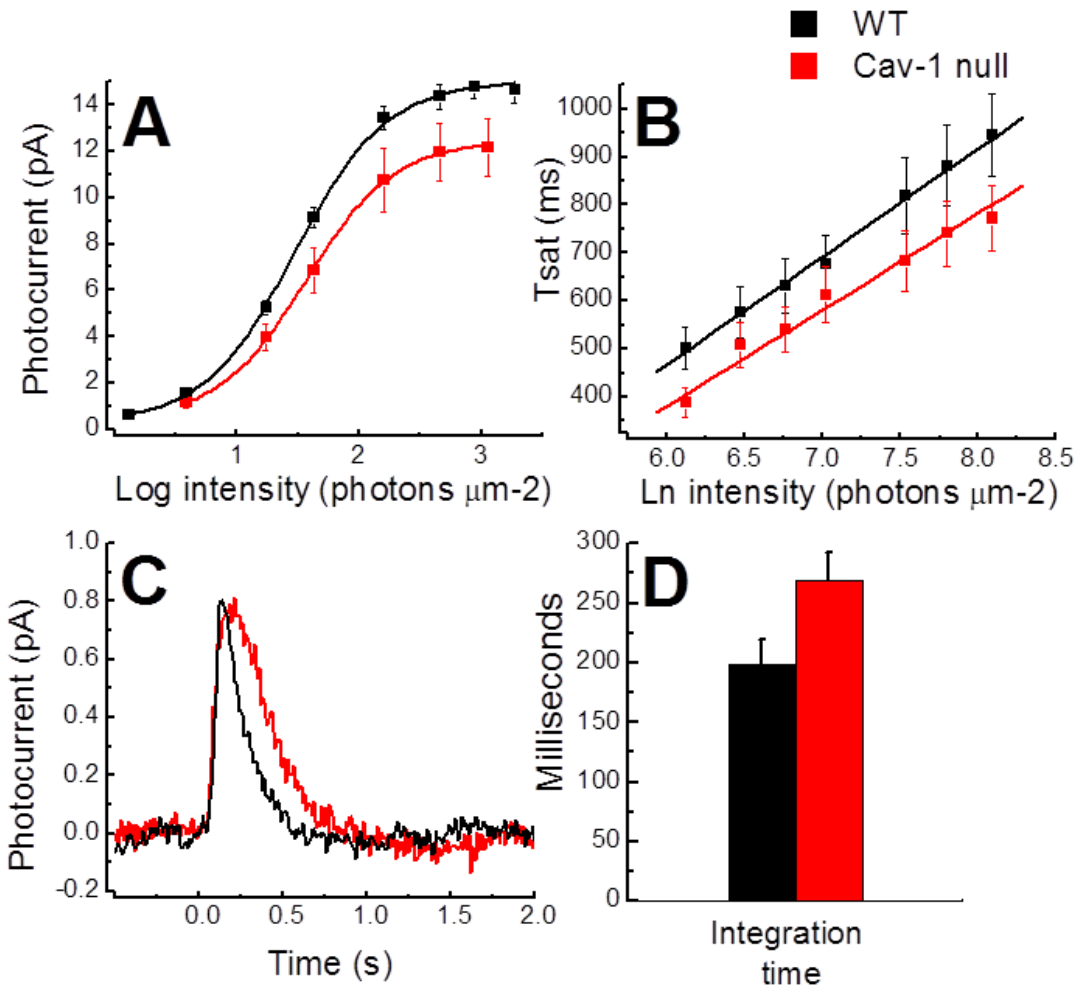

Supplemental Fig. 5. Additional suction electrode recording data from individual *Cav-1* KO and control rod photoreceptors. ***(A)*** Mean intensity-response plots of 45 WT and 8 *Cav-1* KO rods (error bars, SEM). Data were subjected to the Boltzmann equation for curving fitting. The mean half-saturation of the individual rods from WT and *Cav-1* KO mice were not significantly different: 33 photons μm^{-2} for WT (n=45) and 35 photons μm^{-2} for *Cav-1* KO (n = 8). ***(B)*** Time in saturation was estimated by the time it took to return 25 % of the dark current after the channels were closed by the flash and was plotted against natural log of light intensity. The Pepperberg constant, the dominant time constant for response recovery (τ_D), was estimated from the slopes of the lines through the time in saturation. There was no significant difference τ_D between *Cav-1* KO [204 ± 22 ms (n = 9 rods)] and WT rods [211 ± 7 ms (n = 15 rods)]. ***(C)*** Single photon responses calculated from 15 WT rods and 9 *Cav-1* KO rods. Dim light, threshold responses were used in the calculation, which used the variance/mean squared response method. Although the response amplitudes were very close, ~0.8 pA, the *Cav-1* KO rods are somewhat

slower in response kinetics than are WT rods, as indicated by integration time in panel ***(D)***. Integration time, the integral of the current divided by the peak current, assesses the speed of the biochemistry underlying the response. The mean integration time for *Cav-1* KO was 270 ms ± 24 (n = 9) and for WT 199 ± 20 ms (n = 42).

Supplemental Fig. 6.

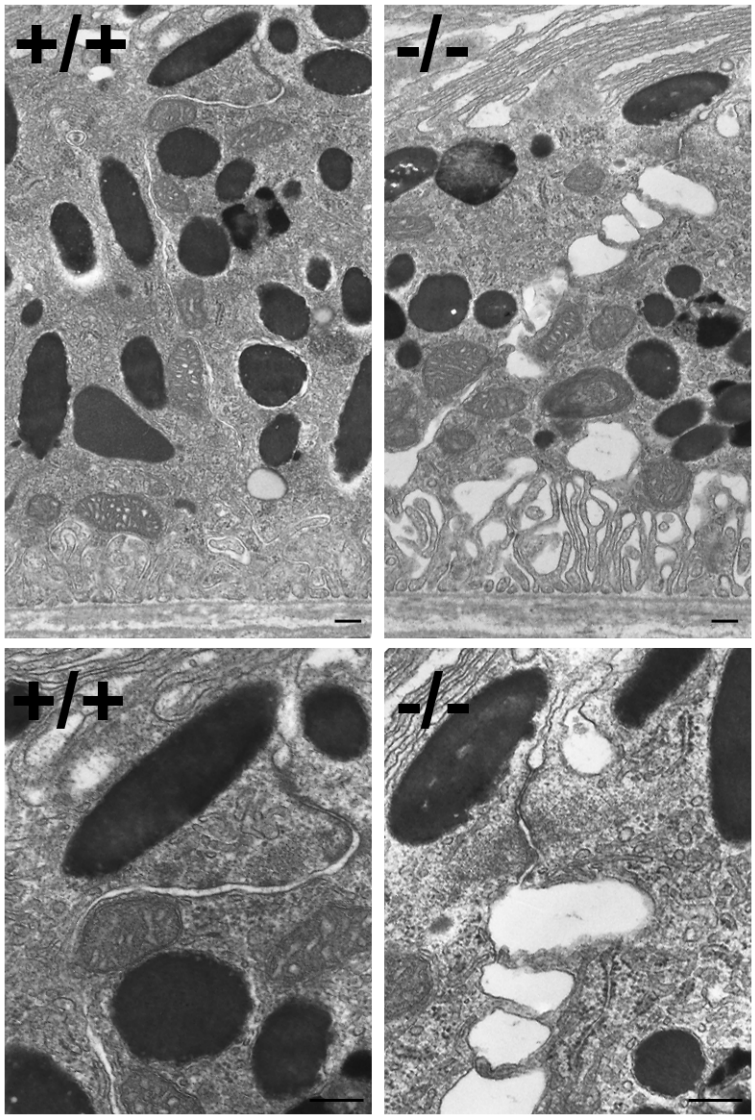

Supplemental Fig. 6. Ultrastructure of RPE from Control and *Cav-1* KO mice. *Cav-1* KO RPE have enlarged spaces between cells and around the basal infoldings (*upper panels*). *Cav-1* KO mice have well-defined tight junctions (*lower right panel*). Scale bar is 500 nm.

Supplemental Table 1: Fatty acid analysis of total lipid extracts from ROS

Fatty Acid	WT	Cav-1 $^{-/-}$
Saturates		
14:0	0.3 ± 0.1	0.43 ± 0.1
16:0	20.1 ± 2.6	19.3 ± 1.9
18:0	22.3 ± 2.0	24.2 ± 2.0
20:0	0.2 ± 0.0	0.2 ± 0.0
22:0	0.1 ± 0.1	0.1 ± 0.1
24:0	less than 0.05	less than 0.05
Monoenoic		
16:1	0.3 ± 0.1	0.3 ± 0.1
18:1	3.7 ± 0.4	3.7 ± 0.4
20:1	0.4 ± 0.2	0.3 ± 0.0
22:1	0.6 ± 0.3	0.9 ± 0.5
24:1	0.2 ± 0.1	0.2 ± 0.2
n6		
18:2n6	0.6 ± 0.1	0.5 ± 0.2
18:3n6	less than 0.05	less than 0.05
20:2n6	0.2 ± 0.2	0.2 ± 0.2
20:3n6	0.4 ± 0.0	0.4 ± 0.1
20:4n6	2.2 ± 0.1	2.3 ± 0.4
22:4n6	0.2 ± 0.1	0.2 ± 0.1
22:5n6	less than 0.05	0.1 ± 0.1
n3		
18:3n3	0.1 ± 0.0	0.1 ± 0.0
20:5n3	0.2 ± 0.0	0.2 ± 0.1
22:5n3	0.6 ± 0.4	0.8 ± 0.1
22:6n3	46.9 ± 4.5	44.6 ± 2.8
n6/n3	0.1 ± 0.0	0.1 ± 0.0

Relative mole percentages (±SD) of fatty acids from total lipid extract of rod outer segment (ROS)